

Can Language Understand Depth?

Renrui Zhang^{*1}, Ziyao Zeng^{*2}, Ziyu Guo¹

¹Peking University ²ShanghaiTech University
1700012927@pku.edu.cn, zengzy@shanghaitech.edu.cn

^{*} indicates equal contributions.

ABSTRACT

Besides image classification, Contrastive Language-Image Pre-training (CLIP) has accomplished extraordinary success for a wide range of vision tasks, including object-level and 3D space understanding. However, it's still challenging to transfer semantic knowledge learned from CLIP into more intricate tasks of quantified targets, such as depth estimation with geometric information. In this paper, we propose to apply CLIP for zero-shot monocular depth estimation, named **DepthCLIP**. We found that the patches of input image could respond to a certain semantic distance token and then be projected to a quantified depth bin for coarse estimation. Without any training, our DepthCLIP surpasses existing unsupervised methods and even approaches the early fully-supervised networks. To our best knowledge, we are the first to conduct zero-shot adaptation from the semantic language knowledge to quantified downstream tasks and perform zero-shot monocular depth estimation. We hope our work could cast a light on the future research. The code is available at <https://github.com/Adonis-galaxy/DepthCLIP>.

CCS CONCEPTS

• Computing methodologies → Neural networks.

KEYWORDS

Contrastive language-Image pre-training, monocular depth estimation, zero-shot prediction

1 INTRODUCTION

Multi-modality learning has long been a fundamental problem, for which a lot of proposed models utilized language knowledge to assist vision tasks and showed inspiring outcomes. Therein, Contrastive Language-Image Pre-Training (CLIP) [19] exerted powerful transfer ability and achieved promising performance on zero/few-shot image classification [6, 28, 31, 33], object detection [21, 34], semantic segmentation [21, 32] and others [29]. Further, for those vision tasks, CLIP is only required to recognize visual signals from a high level, and how to apply its pre-trained semantic language knowledge to quantified vision tasks, e.g., depth estimation, has not been further explored.

Monocular depth estimation is a vital task in the industrial field, which serves as an essential component in various tasks like monocular 3D object detection [15, 25, 30] or point cloud reconstruction from images [26]. It normally relies on dense depth labels to train a network that extracts semantic relations within an image and regresses pixel-wise depth value. However, training networks from scratch supervised by dense labels severely hinders the efficient

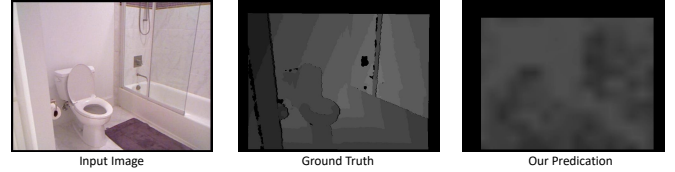


Figure 1: Visualizations of input image, depth ground-truth and the depth estimation of our DepthCLIP. Note that we require no training and directly transfer CLIP [19] for zero-shot prediction.

deployment for application. Also, it is quite costly to collect and annotate the large-scale datasets, such as NYUV2 [23]. Some of the unsupervised methods need extra data like single-view video [16, 27] to capture time-consistent constraint, or demand 3D priors [11] for better spatial modeling. We then ask the question: can we avoid the cost for both training models and collecting data by using semantic language knowledge learned by CLIP [19]?

For the first time, we explore the relationship between language and depth and apply CLIP [19] to monocular depth estimation. CLIP [19] trains an visual encoder and a textual encoder jointly by contrastive loss in the embedding space between both modalities, which narrows the cosine distance of paired image and text features while pushing away the others. The current transfer mode of CLIP only utilizes its pre-trained classification ability, such as classifying each localized object for detection and categorizing each pixel for segmentation. In contrast, during contrastive pre-training, CLIP is not likely to learn knowledge for regressing quantitative values. Thus, it's impossible to directly output depth prediction from the CLIP model for depth estimation. Considering this, we convert the depth value regression to a distance classification task that the CLIP is only required to understand "the object is close/far.", but not "the object is 5 meters away."

In our experiments, we show that the pre-trained CLIP model is able to make responses to the pre-defined distance concepts (like close or remote) for different patches of an image. Then, we map each distance concept to a certain quantitative depth bin and linearly combine the multi-bin depth values weighted by language-patch similarities to produce the depth estimation for a patch. For simplicity, pixels within the same patch would be given the same predicted depth value. By this, our DepthCLIP could conduct zero-shot depth estimation using pre-trained CLIP without any fine-tuning or extra training data, which exceeds existing unsupervised transferred methods and only have a light gap with early fully-supervised models. For analysis, we visualize the distance response of image patches to show that DepthCLIP could coarsely capture the

semantic distance concepts. Besides, we test class-dependent bins to verify that by setting such class-class-dependent bins, DepthCLIP could achieve further improvement for wider practical applications. We summarize our contributions as below:

- We propose DepthCLIP, which is the first to perform zero-shot adaptation from semantic language knowledge to monocular depth estimation task.
- We build the bridge between CLIP’s semantic knowledge and quantified depth value prediction, which casts a light on future research.
- To illustrate our effectiveness, we experiment DepthCLIP on NYU Depth v2 [23], which exceeds existing unsupervised methods and draws near to some fully-supervised models.

2 RELATED WORK

Vision-Language Models. Vision-Language learning has been widely studied and achieved remarkable outcomes to benefit visual representation learning, especially for zero-shot domain transfer in a wide range of downstream tasks. Contemporarily, driven by extensive image-text pairs emerging on the Internet, CLIP [19] and ALIGN [10] have raised a revolution in vision language learning, in which the former uses 400 million noisy image-text pairs and the latter uses 1.8 billion noisy image-text pairs.

CLIP [19] was originally designed for zero-shot image classification. During training, in each batch, CLIP encodes images and corresponding texts into feature space, then maximizes the similarity between corresponding pairs, while minimizing the rest. To conduct zero-shot classification during testing, prompts like “A photo of [class]” would be formed, and the class that has max similarity between prompt features and image features will serve as the prediction. After its remarkable success in zero-shot image classification, it has been applied to few-shot image classification by [6, 28, 31, 33], to image semantic segmentation by [21, 32], and to object detection by [21, 34]. However, solving those tasks requires only the recognition ability. Image classification requires learning generic representation for a single image. Segmentation requires distinguishing between various pixels belonging to different classes (semantic segmentation), objects (instance segmentation), or both (panoptic segmentation). As for object detection, CLIP is only responsible for object-level classification rather than localization. Therefore, no work has been done for CLIP to solve quantified tasks predicting continuous values.

Monocular Depth Estimation. Monocular depth estimation requires estimating pixel-wise depth information from an input single image. Like humans, who directly estimate depth information by parallax, and could infer depth if one eye is blinded by taking advantage of semantics prior learned before. For a computation model, monocular depth estimation is a challenging task due to its lack of stereo information which is the key to solving geometry constrain to obtain depth. As a result, the model could only utilize semantic relationships extracted from the input image and semantic prior learned from training data to roughly estimate depth.

Fully-supervised Methods could learn from ground truth depth map during training to master semantic prior and learn to extract

semantic relationship. DORN [5] trains a deep convolutional neural network while introducing a spacing-increasing discretization strategy to discretize depth and recast depth network learning as an ordinal regression problem. RPSF [18] introduces a differentiable physical model of the aperture mask while simulating the camera imaging pipeline precisely. Due to the recent booming of Transformer architecture in computer vision community [1, 3, 14, 17], some monocular depth estimation models also adopt such structure. For example, ASTransformer [2] designs an Attention-based Up-sample Block to recompense for the texture features, and DepthFormer [13] proposes the hierarchical aggregation and heterogeneous interaction module to build up affinities between features and the model. Fully-supervised methods achieve astonishing performance on monocular depth estimation due to their dedicated designed structure and capacity to model semantics prior of training scenes. However, gathering fully-annotated data would be costly and labor-consuming, which constrains its scalability.

Unsupervised Methods construct pre-text tasks delicately to teach models to discover the semantic affinity within a monocular image. Video could provide temporal consistent constraint for solving geometry, and based on this characteristics, [16, 27] learn depth knowledge from ego-motion of unlabelled monocular video. Besides video, [8] trains itself with widely available binocular stereo images, while exploiting epipolar geometry constraints to generate disparity images and obtain depth predication. Moreover, without using of additional data from other modalities (video or stereo images), [11] introduces plane and line priors to enhance the unsupervised monocular depth estimation. Overall, all previous methods need additional multi-modalities data (video or stereo images) or geometry prior so as to help solve monocular depth estimation. Our work is the first one to use language semantic information learned by CLIP [19] to conduct monocular depth estimation, without the employment of any multi-modalities data or geometry prior.

3 METHOD

As shown in Figure 2, our model utilizes the pre-trained knowledge from CLIP to project the semantic response of each patch into a certain depth bin, and linearly combine those depth values to obtain the final predication. We introduce and discuss three parts respectively below: Image Encoding, Text Encoding, and Depth Projection and Combination.

3.1 Image Encoding

Given a monocular RGB image I , we feed it into the visual encoder without the final pooling layer. Then we acquire its last-layer C -dimensional feature map F_{img} , formulated as,

$$F_{img} = \text{VisualEncoder}(I) \in \mathbb{R}^{HW \times C} \quad (1)$$

Each spot of F_{img} would be given a depth forecast based on its reaction toward semantic language tokens. Since the pre-trained visual encoder of CLIP [19] is received by molding a classification pre-text task, each site of the feature map before pooling would grasp regional semantic information, and pooling would assemble the local knowledge to develop a global interpretation of the given image. As a result, each location of the feature map would preserve

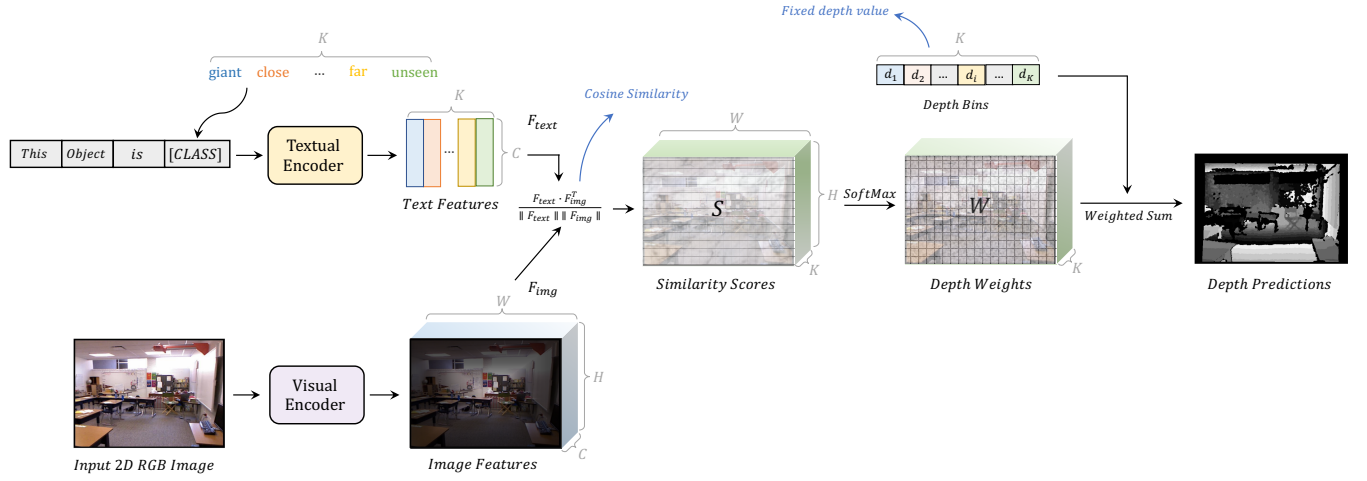


Figure 2: Pipeline of DepthCLIP.

its surrounding semantic details, and be responded to by text token to obtain its depth approximation.

3.2 Text Encoding

Due to the contrastive pre-text task of CLIP, the textual encoder of CLIP [19] would project similar semantic tokens to the neighborhood of image features. In DepthCLIP, we utilize prompts like 'This object is distance class' and apply the semantic tokens close, far, remote that substitute distance class to form K semantic tokens. Those tokens T will pass through the textual encoder of CLIP [19] into latent space by

$$F_{text} = \text{TextualEncoder}(T) \in \mathbb{R}^{K \times C}, \quad (2)$$

where the dimension C equals F_{img} . We then calculate the cosine similarity between semantic tokens' features F_{text} and image features F_{img} to acquire similarity scores by

$$S = \frac{F_{text} \cdot F_{img}^T}{\|F_{text}\| \|F_{img}\|} \in \mathbb{R}^{K \times HW} \quad (3)$$

3.3 Depth Projection and Combination

After obtaining similarity scores S ($dim = H * W * K$), they ought to be cast to quantified depth to receive depth prediction. That is to say, "close" shall be projected to "1m". We apply a temperature softmax function among such similarity scores S to obtained linear combination weight by:

$$W = \frac{e^{S_{:,i}}}{\sum_{j=1}^K e^{S_{:,j}}}, \quad \text{for } i = 1, \dots, K \quad (4)$$

Then, we employ such weights to linearly combined depth bins \mathbf{d} ($dim = K * 1$, like $[d_1=1.00m, d_2=2.00m, d_3=3.00m, \dots]$) to obtain the final depth prediction \mathbf{D}_{pred} ($dim = H * W * 1$) for each location of the image feature map, which is aligned with patches in the image:

$$\mathbf{D}_{pred} = \sum_{i=1}^K \mathbf{W}_{:,i} * \mathbf{d}_i. \quad (5)$$

Where $\mathbf{D}_{pred_{i,j}}$ is the depth of the patch in i th row and j th column. All pixels belonging to such certain patch will be presented with the same depth prediction $\mathbf{D}_{pred_{i,j}}$, where $i \in [1, H], j \in [1, W]$.

4 EXPERIMENTS

To demonstrate the effectiveness of our zero-shot training-free depth estimator, we conduct ample experiments examining different facets of our approach. After introducing the implementation details, we evaluate our methods on a mainstream challenging benchmark—NYU Depth v2 [23]. Ablation studies and visualization are provided to offer a more thorough investigation of our method.

4.1 Datasets

We evaluate our method on NYU Depth v2 [23]. The dataset consists of 120K pairs of RGB and depth images, in which all image pairs are taken by the Microsoft Kinect sensor under 464 indoor scenes with a resolution of 480×640 . Depth range for each pixel is 0-10m. The same training/testing split configuration are applied following [4, 12]. The training set covers 36,253 images from 249 scenes, while the testing set contains 654 images from the remaining 215 scenes. To remove frames, all samples are cropped to the resolution of 416×512 with the identical configuration in [24].

4.2 Implementation Details

We implement our model with the PyTorch framework. Our image and textual encoders employ the pre-trained ResNet-50 [9] of CLIP [19]. For semantic prompts, we tested various kinds of hand-craft prompts, and pick "This object is [distance class]". For semantic distance classes, we investigated diverse combinations and select ['giant', 'extremely close', 'close', 'not in distance', 'a little remote', 'far', 'unseen'], 7 semantic bins in total. Each of which aligns with a depth bin of [1.00, 1.50, 2.00, 2.25, 2.50, 2.75, 3.00]. We set this setting for our main experiments since the range of indoor depth could be properly captured under such proper numbers of semantic

and depth bins. The temperature of the final softmax function is set to 0.1.

4.3 Evaluation Metrics

The evaluation metrics are following previous works [2]. We compare our method quantitatively with metrics listed below: mean absolute relative error (rel), root mean square error (rmse), absolute error in log space (\log_{10}), and threshold accuracy (δ_i). The formula of each metric has been itemized below:

$$\text{rel} = \frac{1}{n} \sum_p \frac{|y_p - \hat{y}_p|}{\hat{y}_p}, \quad \text{rmse} = \sqrt{\frac{1}{n} \sum_p (y_p - \hat{y}_p)^2}$$

$$\log_{10} = \frac{1}{n} \sum_p |\log_{10}(y_p) - \log_{10}(\hat{y}_p)|$$

$$\delta = \% \text{ of } y_p \text{ s.t. } \max\left(\frac{y_p}{\hat{y}_p}, \frac{\hat{y}_p}{y_p}\right) = \delta < \text{thr for } \text{thr} = 1.25, 1.25^2, 1.25^3 \quad (6)$$

4.4 Quantified Results

Table 1 shows our results compared with other monocular depth estimation methods. The table is divided by different supervisions and pre-training datasets. The lower bound is obtained by randomly making predication for each pixel within the depth range 0-10m. It could be noticed that despite the gap between our method with fully-supervised methods, DepthCLIP exceeds the lower bound by a large margin, even surpassing other zero-shot transferring methods that are pre-trained on the dataset especially prepared for monocular depth estimation (unsupervised KITTI monocular video [7]). Besides, the performance of our DepthCLIP has been highly close to some fully-supervised methods like Make3D [22], even exceeding it in terms of rmse (1.186 of ours compared with 1.214 of Make3D [22]).

4.5 Class-dependent Depth Bin

Our DepthCLIP requires attaching a quantified depth bin to each semantic language token, then linearly combined to obtain final predication. Shown as Table 3, images from different classes possess different depth distribution. CLIP [19] can capture semantic distance relationships within one image, but patches holding different distances of various scenes could be mapped to the same semantic concept. In other words, the same semantic token should be mapped to different class-dependent quantified depth bins in different scenes, to achieve better performance. Due to the limit of time, we remain the same bin partition for all classes, and conduct ablation to examine the effectiveness of using class-dependent bin partitioning.

Shown as Table 2, we select the bathroom class, the classroom class, and all classes of NYU Depth v2 [23] to test class-dependent depth bin partitioning. Each depth bin partition is also tested with all classes of NYU Depth v2 [23] to serve as a comparison. We could notice that by depth bin partition based on scene class of test image, compared with evaluating with original shared by all classes for NYU Depth v2 [23] used in Table 1, we could achieve a remarkable performance gain. On the other hand, different classes

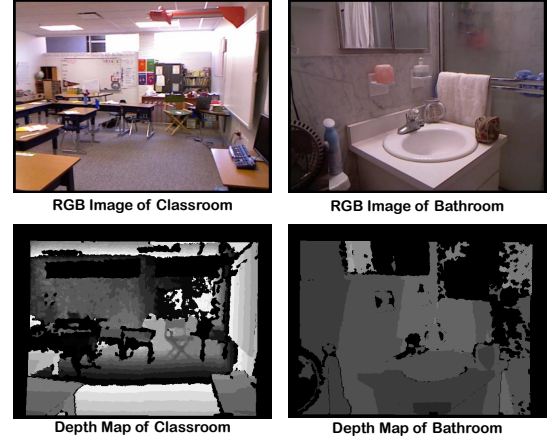


Figure 3: Depth distribution gap between different classes.

have different best bin partitions. That is to say, we could learn a class-dependent bin partition, and conduct zero-shot classification using CLIP [19] to match images with corresponding depth bin partitions to achieve better results, which would be a worthy future research direction.

4.6 Prompt Design

We evaluate our method under different prompt designs on all classes of NYU Depth v2 [23]. Shown as Table 3, our method achieves the best performance under the original prompt design, which is used for the results we report for Table 1. It is worth noticing that, the performance gap among different prompt settings does not vary too much, especially not as sensitive as the depth bin partition shown in Table 2. This outcome is caused by similar semantic meanings inhabiting within different semantic tokens, like "giant" and "extremely close" express a similar meaning, and a patch containing a close object would be projected to both tokens, with only response intensity varying a little for different prompt designs. In this way, the major part of the semantic response score will remain stable across different hand-craft prompt designs. It reveals that our method is robust to hand-craft prompt design, which means it would be time-saving to tune a suitable prompt for our method.

4.7 Semantic Bin Responses

Shown as Figure 4, we visualize semantic bin responses in different patches within one single image, to demonstrate CLIP [19]'s ability to distinguish patches from different distances. Here, the final feature map would be 13×17 , then each patch of such feature map would be given a depth prediction. Each patch has a wide perceptive field during encoding, which enables it to catch surrounding information to decide its distance. Each patch would have its semantic bin responses then be attached to a certain depth and linearly combined to obtain final predication. Detailed correspondence between semantic bins and quantified depth is shown in the orange table. Each patch's response to the semantic bin is shown in the bar chart, and linearly combined predication with ground truth depth label is shown as "GT" and "Pred". We could notice

Method	Pre-training	Supervision	$\delta < 1.25 \uparrow$	$\delta < 1.25^2 \uparrow$	$\delta < 1.25^3 \uparrow$	rel \downarrow	$\log_{10} \downarrow$	rmse \downarrow
Make3D [22]	-	depth	0.447	0.745	0.897	0.349	-	1.214
DORN [5]	-	depth	0.828	0.965	0.992	0.115	0.051	0.509
ASTransformer [2]	-	depth	0.902	0.985	0.997	0.103	0.044	0.374
DepthFormer [13]	-	depth	0.921	0.989	0.998	0.096	0.041	0.339
RPSF [18]	-	depth	0.952	0.989	0.997	0.072	0.029	0.267
Lower Bound	-	-	0.140	0.297	0.471	1.327	0.323	2.934
vid2depth [16]	KITTI video [7]	0-shot	0.268	0.507	0.695	0.572	-	1.637
Zhang et al. [27]	KITTI video [7]	0-shot	0.350	0.617	0.799	0.513	0.529	1.457
DepthCLIP	CLIP [19]	0-shot	0.394	0.683	0.851	0.388	0.156	1.167

Table 1: Performance of Monocular Depth Estimation on NYU Depth v2 [23]. The table is divided by different supervisions and pre-training datasets. Lower bound is obtained by randomly making predication for each pixel within depth range 0-10m.

Bin partition	Depth bin partition details (in meters)					
Original bin	[1.00, 1.50, 2.00, 2.25, 2.50, 2.75, 3.00]					
Class-dependent 1	[1.00, 2.00, 2.25, 2.50, 2.75, 3.00, 4.00]					
Class-dependent 2	[1.00, 1.50, 2.00, 2.50, 3.00, 3.50, 4.00]					
Class-dependent 3	[1.00, 1.25, 1.50, 1.75, 2.00, 2.25, 2.50]					
Class-dependent 4	[2.00, 2.50, 3.00, 3.25, 3.50, 3.75, 4.00]					

Class: Bathroom	$\delta < 1.25 \uparrow$	$\delta < 1.25^2 \uparrow$	$\delta < 1.25^3 \uparrow$	rel \downarrow	$\log_{10} \downarrow$	rmse \downarrow
Original bin	0.333	0.631	0.814	0.549	0.175	0.922
Class-dependent 1	0.248	0.490	0.699	0.754	0.219	1.237
Class-dependent 2	0.236	0.460	0.675	0.801	0.229	1.308
Class-dependent 3	0.425	0.723	0.893	0.373	0.141	0.745
Class-dependent 4	0.129	0.302	0.535	1.072	0.287	1.682
Best partition's gain	+0.092	+0.092	+0.079	-0.176	-0.034	-0.177

Class: Classroom	$\delta < 1.25 \uparrow$	$\delta < 1.25^2 \uparrow$	$\delta < 1.25^3 \uparrow$	rel \downarrow	$\log_{10} \downarrow$	rmse \downarrow
Original bin	0.308	0.533	0.742	0.372	0.193	1.826
Class-dependent 1	0.312	0.565	0.820	0.383	0.179	1.694
Class-dependent 2	0.310	0.583	0.830	0.397	0.175	1.636
Class-dependent 3	0.231	0.452	0.600	0.407	0.246	2.138
Class-dependent 4	0.276	0.637	0.844	0.461	0.173	1.544
Best partition's gain	-0.032	+0.104	+0.102	+0.088	-0.020	-0.282

Class: All	$\delta < 1.25 \uparrow$	$\delta < 1.25^2 \uparrow$	$\delta < 1.25^3 \uparrow$	rel \downarrow	$\log_{10} \downarrow$	rmse \downarrow
Original bin	0.394	0.683	0.851	0.388	0.156	1.167
Class-dependent 1	0.373	0.653	0.828	0.467	0.166	1.228
Class-dependent 2	0.366	0.641	0.819	0.496	0.170	1.248
Class-dependent 3	0.333	0.621	0.818	0.353	0.176	1.290
Class-dependent 4	0.288	0.548	0.752	0.663	0.201	1.439
Best partition's gain	-	-	-	-	-	-

Table 2: Ablations of class-dependent depth bin. Perform in bathroom, classroom, and all classes of NYU Depth v2 [23]. The uppermost table shows partition details of each depth bin partition, the lower three tables show the performance of each partition in the bathroom, classroom, and all classes. The original bin is the one used for Table 1 to evaluate the entire dataset among all classes. Performance gain between the original bin and best class-dependent bin is listed in the last row, while the best class-dependent bin is bold.



Figure 4: Semantic bin responses in different patches of an image for DepthCLIP.

a significant difference in semantic response for close patch and distant patch, which forms the foundation of the effectiveness of our DepthCLIP.

4.8 Depth Predication Visualization

As shown in Figure5, we visualize depth predictions of our DepthCLIP, compared with ground truth and input RGB images. It could be witnessed that our prediction is a little bit blurred, and focus more on detailed objects, like the tap on the left column, and the closetool as well as the bathtub on the right column. This is discussed in the limitation section below, that the visual encoder of CLIP [19] is pre-trained using a classification pre-text task, in which the model pays more attention to local details that help classification, like furniture. In this way, backgrounds and local areas would be neglected.

5 LIMITATIONS & FUTURE RESEARCH DIRECTION

One limitation is that our work requires hand-craft depth bin tuning. For various depth distributions of different scenes, DepthCLIP would perform poorly if different scenes share the same depth

Prompt number	Prompt design details (in semantic token words)
Original prompt	[giant, extremely close, close, not in distance, a little remote, far, unseen]
Prompt 1	[extremely close, close, middle, a little far, far, quite far, unseen]
Prompt 2	[extremely close, very close, close, a little close, a little far, far, unseen]
Prompt 3	[giant, close, a little close, not in distance, a bit remote, far, unseen]

Prompt number	$\delta < 1.25 \uparrow$	$\delta < 1.25^2 \uparrow$	$\delta < 1.25^3 \uparrow$	rel \downarrow	$\log_{10} \downarrow$	rmse \downarrow
Original prompt	0.394	0.683	0.851	0.388	0.156	1.167
Prompt 1	0.341	0.623	0.816	0.379	0.175	1.274
Prompt 2	0.377	0.667	0.845	0.385	0.161	1.196
Prompt 3	0.380	0.670	0.846	0.375	0.160	1.196

Table 3: Ablations of prompt design. Perform in all classes of NYU Depth v2 [23]. The upper table shows partition detailed semantic token words of prompt design, the lower table shows the performance of each prompt design in all classes. The original prompt design is the one used for Table 1 to evaluate the entire dataset among all classes, which is the best among all those evaluated designs. The best prompt design is bold.

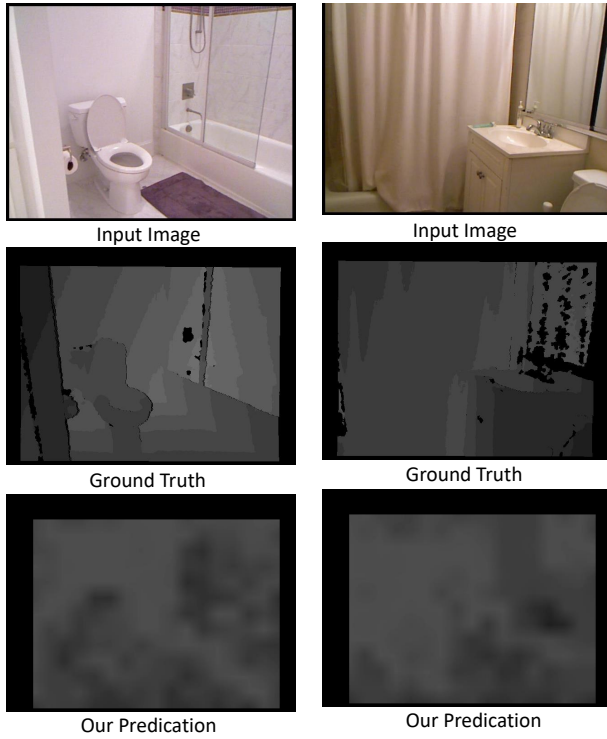


Figure 5: Depth predication visualization, compared with ground truth and input RGB image.

bin setting. One possible solution is to conduct zero-shot image classification first, which could naturally be done by CLIP [19], then determine class-dependent depth bins for predicated scene class. However, such a class-dependent depth bin still requires tuning, which would be labor-consuming. Therefore, learning class-dependent depth bins for each predicated scene class would be a worthwhile future direction. Given the significance of using

class-dependent depth bins shown in Table 3, if we could learn class-dependent depth bins automatically and effectively, zero-shot monocular depth estimation would achieve remarkable improvement and would be efficiently adapted to various scenes sharing different depth distributions, like from road to the warehouse.

Another limitation of DepthCLIP is that its visual encoder of CLIP [19] is trained under a classification pre-text task, in which the local region would be processed and pooled into a global feature for classification. As a result, its visual encoder would pay more attention to local details which help identify its scene class, like furniture. Local regions without noteworthy features for classification would not be fully extracted by the visual encoder. Under such circumstances, DepthCLIP would have non-significant semantic depth reactions for background regions, like large areas of wall, ceiling, or floor. Such an issue is naturally owned by CLIP [19], and is possessed by all methods which would exploit features that are useless for image classification pre-training of CLIP [19], like the attributes entanglement and inaccuracy in word generation mentioned in DALL-E 2[20]. For such a universal weakness, one possible solution is to train a vision language model with a regional pre-text task like image segmentation or object detection, to drive more regions' sensitivity.

6 CONCLUSION

In this paper, we propose DepthCLIP to conduct zero-shot monocular depth estimation with Contrastive Language-Image Pre-Training, which discards the need of training and data with depth labels. It directly applies CLIP [19] that only pre-trained with large-scale image-text pairs to monocular depth estimation task, and achieved satisfying performance. We hope our work could cast a light on the research of bridging semantic vision language knowledge to quantitative vision tasks, and open future research on zero-shot monocular depth estimation.

REFERENCES

- [1] Nicolas Carion, Francisco Massa, Gabriel Synnaeve, Nicolas Usunier, Alexander Kirillov, and Sergey Zagoruyko. 2020. End-to-end object detection with transformers. In *European conference on computer vision*. Springer, 213–229.
- [2] Wenjie Chang, Yueyi Zhang, and Zhiwei Xiong. 2021. Transformer-based Monocular Depth Estimation with Attention Supervision. (2021).
- [3] Alexey Dosovitskiy, Lucas Beyer, Alexander Kolesnikov, Dirk Weissenborn, Xiuhua Zhai, Thomas Unterthiner, Mostafa Dehghani, Matthias Minderer, Georg Heigold, Sylvain Gelly, et al. 2020. An image is worth 16x16 words: Transformers for image recognition at scale. *arXiv preprint arXiv:2010.11929* (2020).
- [4] David Eigen, Christian Puhrsch, and Rob Fergus. 2014. Depth map prediction from a single image using a multi-scale deep network. *Advances in neural information processing systems* 27 (2014).
- [5] Huan Fu, Mingming Gong, Chaohui Wang, Kayhan Batmanghelich, and Dacheng Tao. 2018. Deep ordinal regression network for monocular depth estimation. In *Proceedings of the IEEE conference on computer vision and pattern recognition*. 2002–2011.
- [6] Peng Gao, Shijie Geng, Renrui Zhang, Teli Ma, Rongyao Fang, Yongfeng Zhang, Hongsheng Li, and Yu Qiao. 2021. Clip-adapter: Better vision-language models with feature adapters. *arXiv preprint arXiv:2110.04544* (2021).
- [7] Andreas Geiger, Philip Lenz, Christoph Stiller, and Raquel Urtasun. 2013. Vision meets robotics: The kitti dataset. *The International Journal of Robotics Research* 32, 11 (2013), 1231–1237.
- [8] Clément Godard, Oisin Mac Aodha, and Gabriel J Brostow. 2017. Unsupervised monocular depth estimation with left-right consistency. In *Proceedings of the IEEE conference on computer vision and pattern recognition*. 270–279.
- [9] Kaiming He, Xiangyu Zhang, Shaoqing Ren, and Jian Sun. 2016. Deep residual learning for image recognition. In *Proceedings of the IEEE conference on computer vision and pattern recognition*. 770–778.
- [10] Chao Jia, Yinfei Yang, Ye Xia, Yi-Ting Chen, Zarana Parekh, Hieu Pham, Quoc Le, Yun-Hsuan Sung, Zhen Li, and Tom Duerig. 2021. Scaling up visual and vision-language representation learning with noisy text supervision. In *International Conference on Machine Learning*. PMLR, 4904–4916.
- [11] Hualie Jiang, Laiyan Ding, Junjie Hu, and Rui Huang. 2021. PLNet: Plane and Line Priors for Unsupervised Indoor Depth Estimation. In *2021 International Conference on 3D Vision (3DV)*. IEEE, 741–750.
- [12] Jin Han Lee, Myung-Kyu Han, Dong Wook Ko, and Il Hong Suh. 2019. From big to small: Multi-scale local planar guidance for monocular depth estimation. *arXiv preprint arXiv:1907.10326* (2019).
- [13] Zhenyu Li, Zehui Chen, Xianming Liu, and Junjun Jiang. 2022. DepthFormer: Exploiting Long-Range Correlation and Local Information for Accurate Monocular Depth Estimation. *arXiv preprint arXiv:2203.14211* (2022).
- [14] Ze Liu, Yutong Lin, Yue Cao, Han Hu, Yixuan Wei, Zheng Zhang, Stephen Lin, and Baining Guo. 2021. Swin transformer: Hierarchical vision transformer using shifted windows. In *Proceedings of the IEEE/CVF International Conference on Computer Vision*. 10012–10022.
- [15] Zechen Liu, Zizhang Wu, and Roland Tóth. 2020. Smoke: Single-stage monocular 3d object detection via keypoint estimation. In *Proceedings of the IEEE/CVF Conference on Computer Vision and Pattern Recognition Workshops*. 996–997.
- [16] Reza Mahjourian, Martin Wicke, and Anelia Angelova. 2018. Unsupervised learning of depth and ego-motion from monocular video using 3d geometric constraints. In *Proceedings of the IEEE conference on computer vision and pattern recognition*. 5667–5675.
- [17] Mingyuan Mao, Renrui Zhang, Honghui Zheng, Teli Ma, Yan Peng, Errui Ding, Baochang Zhang, Shumin Han, et al. 2021. Dual-stream network for visual recognition. *Advances in Neural Information Processing Systems* 34 (2021).
- [18] Mazen Mel, Muhammad Siddiqui, and Pietro Zanuttigh. 2022. End-to-end Learning for Joint Depth and Image Reconstruction from Diffracted Rotation. *arXiv preprint arXiv:2204.07076* (2022).
- [19] Alec Radford, Jong Wook Kim, Chris Hallacy, Aditya Ramesh, Gabriel Goh, Sandhini Agarwal, Girish Sastry, Amanda Askell, Pamela Mishkin, Jack Clark, et al. 2021. Learning transferable visual models from natural language supervision. In *International Conference on Machine Learning*. PMLR, 8748–8763.
- [20] Aditya Ramesh, Prafulla Dhariwal, Alex Nichol, Casey Chu, and Mark Chen. 2022. Hierarchical text-conditional image generation with clip latents. *arXiv preprint arXiv:2204.06125* (2022).
- [21] Yongming Rao, Wenliang Zhao, Guangyi Chen, Yansong Tang, Zheng Zhu, Guan Huang, Jie Zhou, and Jiwen Lu. 2021. DenseCLIP: Language-Guided Dense Prediction with Context-Aware Prompting. *arXiv preprint arXiv:2112.01518* (2021).
- [22] Ashutosh Saxena, Min Sun, and Andrew Y Ng. 2008. Make3D: Depth Perception from a Single Still Image.. In *Aaai*, Vol. 3. 1571–1576.
- [23] Nathan Silberman, Derek Hoiem, Pushmeet Kohli, and Rob Fergus. 2012. Indoor segmentation and support inference from rgb-d images. In *European conference on computer vision*. Springer, 746–760.
- [24] Minsoo Song, Seokjae Lim, and Wonjun Kim. 2021. Monocular depth estimation using laplacian pyramid-based depth residuals. *IEEE transactions on circuits and systems for video technology* 31, 11 (2021), 4381–4393.
- [25] Tai Wang, Xinge Zhu, Jiangmiao Pang, and Dahua Lin. 2021. Fcos3d: Fully convolutional one-stage monocular 3d object detection. In *Proceedings of the IEEE/CVF International Conference on Computer Vision*. 913–922.
- [26] Wei Zeng, Sezer Karaoglu, and Theo Gevers. 2018. Inferring point clouds from single monocular images by depth intermediation. *arXiv preprint arXiv:1812.01402* (2018).
- [27] Mingliang Zhang, Xinchun Ye, Xin Fan, and Wei Zhong. 2020. Unsupervised depth estimation from monocular videos with hybrid geometric-refined loss and contextual attention. *Neurocomputing* 379 (2020), 250–261.
- [28] Renrui Zhang, Rongyao Fang, Peng Gao, Wei Zhang, Kunchang Li, Jifeng Dai, Yu Qiao, and Hongsheng Li. 2021. Tip-Adapter: Training-free CLIP-Adapter for Better Vision-Language Modeling. *arXiv preprint arXiv:2111.03930* (2021).
- [29] Renrui Zhang, Ziyu Guo, Wei Zhang, Kunchang Li, Xupeng Miao, Bin Cui, Yu Qiao, Peng Gao, and Hongsheng Li. 2022. Pointclip: Point cloud understanding by clip. In *Proceedings of the IEEE/CVF Conference on Computer Vision and Pattern Recognition*. 8552–8562.
- [30] Renrui Zhang, Han Qiu, Tai Wang, Xuanzhuo Xu, Ziyu Guo, Yu Qiao, Peng Gao, and Hongsheng Li. 2022. MonoDETR: Depth-aware Transformer for Monocular 3D Object Detection. *arXiv preprint arXiv:2203.13310* (2022).
- [31] Renrui Zhang, Longtian Qiu, Wei Zhang, and Ziyao Zeng. 2021. VT-CLIP: Enhancing Vision-Language Models with Visual-guided Texts. *arXiv preprint arXiv:2112.02399* (2021).
- [32] Chong Zhou, Chen Change Loy, and Bo Dai. 2021. DenseCLIP: Extract Free Dense Labels from CLIP. *arXiv preprint arXiv:2112.01071* (2021).
- [33] Kaiyang Zhou, Jingkang Yang, Chen Change Loy, and Ziwei Liu. 2021. Learning to prompt for vision-language models. *arXiv preprint arXiv:2109.01134* (2021).
- [34] Xingyi Zhou, Rohit Girdhar, Armand Joulin, Phillip Krähenbühl, and Ishan Misra. 2022. Detecting Twenty-thousand Classes using Image-level Supervision. *arXiv preprint arXiv:2201.02605* (2022).